A Dynamic Mode Decomposition Predictive Control scheme for an Osmotic Membrane Distillation Process

Francesco Giannini
Dept. of Environmental Engineering
University of Calabria
Rende, CS, Italy
francescogiannini97@libero.it
0000-0001-5892-2049

Efrem Curcio
Dept. of Environmental Engineering
University of Calabria
Rende, CS, Italy
efrem.curcio@unical.it
0000-0001-7497-878X

Pietro Argurio
Dept. of Environmental Engineering
University of Calabria
Rende, CS, Italy
pietro.argurio@unical.it
0000-0002-5656-4986

***Abstract*—In this paper, a Data-Driven predictive control strategy is proposed for the regulation of the transmembrane flux in an Osmotic Membrane Distillation (OMD) lab-scale unit operating with a sucrose solution as feed and $MgCl_2$ as hypersaline draw solution. The control objective is to accurately track desired flux setpoints under the intrinsic nonlinearities of the underlying mass and heat transport phenomena. To this end, physicochemical laws are combined with experimental data to develop a digital twin of the process. Such digital twin allows the collection of simulated informative data to compute a linear description of the plant system in a data-driven fashion. In particular, the proposed approach is based on the Dynamic Mode Decomposition with Control (DMDc) algorithm. The identified model is then embedded within a predictive control scheme, allowing the constrained regulation of the unit. Numerical simulations demonstrate the effectiveness of the proposed method in driving the system toward multiple operating points while ensuring accurate flux regulation.**

***Index Terms*—Dynamic Mode Decomposition, Model Predictive Control, Digital Twin, Membrane distillation process.**

I. Introduction

Nowadays, one of the most important research lines in Control Theory is Data-Driven Control [1]. Many results in this framework are based on the Koopman theory [2]. The main advantage behind this theory is the formal proof that it is possible to represent a nonlinear dynamical system in terms of an infinite-dimensional linear operator - named Koopman operator - acting on a Hilbert space of measurement functions of the state of the system. One mileston result in this change of paradigm is [3], where the author applied Koopman theory to discuss the properties of finite-dimensional projections. Initially applied to fluid-flow decompositions [4], the Koopman operator recently has been widely used in control applications [5], [6] The difficulty in its use stands on the fact that its exact closed form is hard to obtain [8].

A finite-dimensional approximation of the Koopman operator can be computed through Dynamic Mode Decomposition (DMD) [9]. Originally proposed for autonomous systems, it has been extended to take into account the effect of control inputs in [7]. There, the Data-driven method named Dynamic Mode Decomposition with control (DMDc) has been introduced and validated [7].

This paper proposes a control strategy based on DMDc in the challenging environment of Osmotic Membrane Distillation (OMD) [10]. OMD is a membrane contactor process in which mass transport occurs across a microporous hydrophobic membrane that provides physical support to vapor–liquid equilibrium interfaces. Driven by the vapor partial pressure gradient, water vapor diffuses through the membrane from the high water-activity side (feed solution) to the low water-activity side (draw solution). Both compartments are maintained at the same constant bulk temperature; therefore, mass transfer proceeds under quasi-isothermal conditions and with moderate transmembrane flux generally resulting in negligible impact of concentration and temperature polarization phenomena. Compared with thermally driven membrane distillation, OMD offers the advantage of operation at near-ambient temperature, which enables the dehydration of thermolabile solutes, such as biomolecules and food constituents, while minimizing thermal degradation and preserving functional properties [11] [12].

This paper addresses the data-driven modeling and control of a laboratory-scale OMD unit exhibiting strongly nonlinear dynamics arising from the coupling of heat and mass transport phenomena. Experimental measurements are integrated with first-principles physicochemical modeling to develop a digital twin capable of reproducing the observed behavior of the membrane module. In parallel, a linear approximation of the underlying nonlinear dynamics is identified using the DMDc algorithm. The resulting linear model is shown to capture the dominant dynamical features of the process within the operating region of interest. The digital twin is subsequently employed as a reference framework to extensively validate the accuracy and predictive capabilities of the identified model under different operating conditions. Building upon this validated representation, this linear formulation is integrated within a model predictive control (MPC) [13] scheme to enable prediction-based regulation of the system dynamics.

TABLE I
PHYSICOCHEMICAL CONSTANTS

Parameter	Meaning	Unit	Value
R	Gas constant	$[Pa\,m^3K^{-1}mol^{-1}]$	8.31
T_{avg}	Environmental temperature	$[K]$	293
$D^k_{w,e}$	Effective Knudsen diffusion coeff.	$[m^2/s]$	$2.1075 \cdot 10^{-5}$
$D^0_{w-air,e}$	Effective molecular diffusion coeff.	$[m^2/s]$	$1.3033 \cdot 10^{-5}$
P_{tot}	Standard pressure	$[Pa]$	101325

TABLE II
PARAMETERS

Parameter	Meaning	Unit	Value
A	Area of the membrane	$[cm^2]$	120
δ	Thickness of the membrane	$[mm]$	0.17
n^f	Sucrose in the feed (constant)	$[mol]$	0.0876
$n^f_{H_2O}(t=0)$	Initial water in the feed	$[mol]$	3.8856
n^d	$MgCl_2$ in the draw (constant)	$[mol]$	3
$n^d_{H_2O}(t=0)$	Initial water in the draw	$[mol]$	55.5
$p^{*,0}_w$	Vapor pressure of pure water	$[Pa]$	$2.3296 \cdot 10^3$

The reported results demonstrate that the proposed modeling and control framework successfully stabilizes the system around a prescribed transmembrane flow value, highlighting the effectiveness of the identified model in supporting control design for a highly nonlinear process.

An analogous result has been proposed in [14]. The main difference between the two control schemes is that there the data-driven plant representation is based on a robust description, while here DMD provides a single linear model.

The paper outline is hereafter summarized. After a brief recap of notation and basic definition, the following section introduces the integration between data and known physicochemical laws used to build the digital twin of the membrane-distillation process. In section III, the DMDc is resumed and applied to the proposed case-study. Section IV presents the proposed control scheme. Section V provides numerical results on the effectiveness of the methodology. Final considerations conclude the paper.

NOTATION AND DEFINITIONS

The symbol $\mathbb{N}$ denotes the set of natural numbers, $\mathbb{R}$ real numbers, $\mathbb{R}^+$ real numbers greater than 0.

The time is indicated as $t \in \mathbb{R}^+$ or as $k \in \mathbb{N}$. The difference between these two notations is that while the equations governing real world are defined as functions of the continuous time, digital controllers are defined as algorithms. Moreover, data are assumed to be available only at given time instants $t = kT$, where T is the sampling time.

Given a vector $v \in \mathbb{R}^n$, its euclidean norm is denoted as $||v||$, while the notation $v(k_1 : k_2)$ denotes the vector extracted from v containing its elements from the index k_1 to k_2.

Table I resumes all the physicochemical constants that are used in the paper; table II resumes the parameters of the process.

II. OMD PROCESS

The OMD process is described by the following mathematical model, derived under the assumption of negligible concentration and temperature polarization effects, as discussed above.

$$\begin{cases} \frac{dV^f(t)}{dt} = -J_w(t)A \\ \frac{dV^d(t)}{dt} = J_w(t)A + u(t) \end{cases} \tag{1}$$

Here, the control input $u(t) \in \mathbb{R}$ resumes the simultaneous effect of removing volume from the draw solution and adding from a make-up solution with known higher concentration. The other terms in (1) are $V^f(t)$, the volume of the feed solution; $V^d(t)$, the volume of the draw solution; and J_w, the transmembrane flux of water vapor. In the autonomous evolution of the process, J_w induces a progressive reduction of the feed volume ($V^f(t)$) and a corresponding increase of the draw-solution volume ($V^d(t)$), where the transferred vapor condenses. The consequent increase in solute concentration in the feed and the concomitant dilution of the draw solution lead to a progressive decline of the mass-transfer driving force over time. J_w can be expressed as:

$$J_w(t) = a_1\left(\frac{1}{D^k_{w,e}} + \frac{y_{air}(t)}{D^0_{w-air,e}}\right)^{-1}\left(p^{d*}_w(t) - p^{f*}_w(t)\right) \tag{2}$$

where:

- the coefficient a_1 is defined as $a_1 := -\frac{1}{\delta R T^m_{avg}}$,
- The molar fraction of air in the membrane can be expressed as:

$$y_{air}(t) = \frac{P_{tot} - \left(\frac{p^{d*}_w(t) + p^{f*}_w(t)}{2}\right)}{P_{tot}} \tag{3}$$

- the vapor pressures are described as:

$$\begin{cases} p^{d*}_w = p^{*,0}_w x^d_w \gamma^{d*}_w \\ p^{f*}_w = p^{*,0}_w x^f_w \gamma^{f*}_w \end{cases} \tag{4}$$

The activity coefficients γ^*_w and the molar fractions $x_w(t)$ have been characterized as resumed in the next two subsections.

A. Feed solution - Aqueous glucose solution

During the osmotic membrane distillation, the sucrose concentration in feed evolves as:

$$\frac{d(c^f(t)V^f(t))}{dt} = 0 \tag{5}$$

where $c^f(t)$ is expressed in $[mol/L]$.

The density of the feed solution has been identified via experimental data and is represented by a linear relationship with respect to the number of moles of water $n^f_{H_2O}(t)$. The resulting model expression is reported in the following:

$$\rho^f(n^f_{H_2O}) = \frac{0.0055 \cdot 30[g]}{30[g] + n^f_{H_2O} \cdot 18.01528[g/mol]} + 0.9729 \tag{6}$$

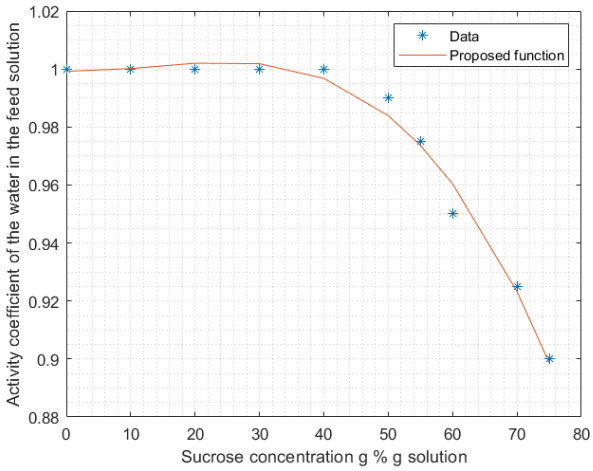

Fig. 1. Interpolation of activity coefficient data in the feed solution

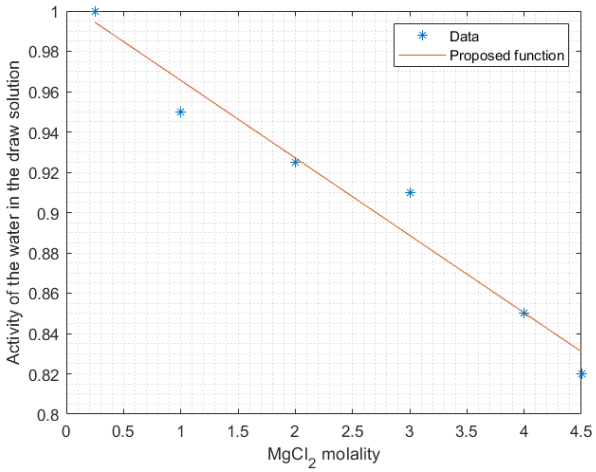

Fig. 2. Interpolation of activity data in the draw solution

The activity coefficient of water in the feed solution (see Fig. 1) is modeled as a function of the number of moles of water $n^f_{H_2O}(t)$, as reported below:

$$\begin{aligned}\gamma^{f*}_w(n^f_{H_2O}) &= -4.828\cdot 10^{-7}\left(\frac{30[g]}{30[g]+n^f_{H_2O}\cdot 18.01528[g/mol]}\right)^3+\\ &+1.897\cdot 10^{-5}\left(\frac{30[g]}{30[g]+n^f_{H_2O}\cdot 18.01528[g/mol]}\right)^2+\\ &+\frac{-4.71\cdot 10^{-5}\cdot 30[g]}{30[g]+n^f_{H_2O}\cdot 18.01528[g/mol]}+0.9992\end{aligned} \tag{7}$$

Source of the data is [15].

Another important parameter is the molar fraction of the water:

$$x^f_w(t)=\frac{n^f_{H_2O}(t)}{n^f_{H_2O}(t)+n^f} \tag{8}$$

B. Draw solution - Aqueous $MgCl_2$ solution

Similarly to the case of the feed solution, the salt concentration in draw tank evolves as:

$$\frac{d(c^d(t)V^d(t))}{dt}=u(t) \tag{9}$$

The density of the draw solution has been identified and can be expressed as a function of the moles of water $n^d_{H_2O}(t)$:

$$\rho^d(n^d_{H_2O})=\left(\frac{10.78[mol]}{n^d_{H_2O}.}+1.003\right)[g/mL] \tag{10}$$

The relation between the molality m (expressed in $[mol/Kg]$) and the activity of the water in the draw solution has been identified and the following linear function obtained, represented in Fig. 2:

$$\gamma^{d*}_w x^d_w(t)=\frac{-0.03844\cdot 3[mol]\rho^d(n^d_{H_2O})}{285.633[g]+n^d_{H_2O}18.01528[g/mol]}+1.004 \tag{11}$$

Source of the data is [16]

The molar fraction of the water in the draw solution is

$$x^d_w(t)=\frac{n^d_{H_2O}(t)}{n^d_{H_2O}(t)+n^d} \tag{12}$$

III. A BRIEF OVERVIEW OF KOOPMAN THEORY AND DMDC

As introduced, the aim of this paper is to integrate the proposed digital twin of our plant with a predictive control scheme based on the approximation of the Koopman operator given by DMDc. This theoretical framework relies on the following assumption about the unknown dynamic evolution of the plant generating the given data:

$$\begin{cases}x(k+1)=f(x(k),u(k))\\ y(k)=g(x(k))\end{cases} \tag{13}$$

here, $x\in\mathbb{R}^n$ is the state, $y\in\mathbb{R}^p$ the measured output and $f(\cdot,\cdot)$, $g(\cdot)$ two functions describing the dynamics, supposed to be unknown. Moreover, no hypothesis about the size of the state-space is considered. The Koopman operator allows to compute the advance from a measure to the next one [1]:

$$\mathcal{K}g(x(k)):=g(f(x(k))=g(x(k+1)) \tag{14}$$

In our experimental setup, we measure the two volumes of the draw and feed solutions, the corresponding concentration, and the trans-membrane flux:

$$y(k)=\begin{bmatrix}c^f(k)\\ c^d(k)\\ V^f(k)\\ V^d(k)\\ J_w(k)\end{bmatrix} \tag{15}$$

DMDc [8] approximates the Koopman operator by means of data $w^d:=\{y(0),u(0),y(1),u(1),y(2),\dots y(N)\}$ collected as:

$$\begin{cases} Y^+ := \begin{bmatrix} y(1) & y(2) & \dots & y(N) \end{bmatrix} \\ Y := \begin{bmatrix} y(0) & y(1) & \dots & y(N-1) \end{bmatrix} \\ U := \begin{bmatrix} u(0) & u(1) & \dots & u(N-1) \end{bmatrix} \end{cases}, \ \Omega := \begin{bmatrix} Y \\ U \end{bmatrix} \tag{16}$$

Once the data are collected as in (16), compute the following Singular Value Decompositions (SVD):

$$\begin{cases} \Omega \approx \tilde{U}\tilde{\Sigma}\tilde{V}^* = \begin{bmatrix} \tilde{U}_1 \\ \tilde{U}_2 \end{bmatrix} \tilde{\Sigma}\tilde{\mathbf{V}} \\ Y^+ \approx \hat{U}\hat{\Sigma}\hat{V}^* \end{cases} \tag{17}$$

Notice that, as in [1], the matrix $\tilde{U}$ has been split into two matrices $\tilde{U} = \begin{bmatrix} \tilde{U}_1 \\ \tilde{U}_2 \end{bmatrix}$, to provide bases for Y and U and that the matrices are truncated to rank r in order to filter noise and capture dominant dynamics.

Finally, assuming that in the lifted space:

$$z(k) := \hat{U}^* y(k) \tag{18}$$

the dynamic of the system can be considered as linear:

$$z(k+1) \approx \tilde{\Phi} z(k) + \tilde{G} u(k) \tag{19}$$

the matrices Φ and G can be identified as following:

$$\begin{cases} \tilde{\Phi} = \hat{U}^* Y^+ \tilde{V} \tilde{\Sigma}^{-1} \tilde{U}_1^* \hat{U} \\ \tilde{G} = \hat{U}^* Y^+ \tilde{V} \tilde{\Sigma}^{-1} \tilde{U}_2^* \end{cases} \tag{20}$$

IV. Control scheme

Based on the above developments, an MPC scheme in the lifted space is proposed, as expressed in the following computable algorithm.

DMDc- based MPC

Initialization

Collect the data w^d;
Stack the data as in (16);
Compute $\tilde{\Phi}$ and $\tilde{G}$ as in (20);

For *each sampling time* k :

1: **Measure** $y(k)$.
2: **Project** the vector $y(k)$ into the lifted space:

$$z(k) = \hat{U}^* y(k) \tag{21}$$

3: **Solve** the following optimization problem:

$$u^{opt} := arg \min_{u=\{u(k+i)\}_{i=0}^{h-1}} \mathcal{L}(z(k), u) \tag{22a}$$

$$s.t.\ z(i+1) = \tilde{\Phi} z(i) + G u(i) \tag{22b}$$

$$u_{min} \leq u(i) \leq u_{max} \tag{22c}$$

$$y_{min} \leq y(i) \leq y_{max} \tag{22d}$$

$$z(k+1) = \tilde{\Phi} z(k) + \tilde{G} u(k)$$

4: **Apply** $u(k) = u^{opt}(1)$ to the plant.

The cost $\mathcal{L}(z(k), u)$ in (22a) is defined as:

$$\mathcal{L}(z(k), u) = \sum_{i=0}^{h-1} \begin{array}{l} ((z(k+i) - z^{ref})' Q^z (z(k+i) - z^{ref}) + \\ + u(k+i)' Q^u u(k+i)) \end{array} \tag{23}$$

where h is the prediction horizon, z^{ref} the desired reference to be tracked.

The constraint (22c) is introduced to explicitly account for the physical limitations of the actuation, ensuring that the control actions computed by the predictive controller remain implementable in practice. Similarly, the additional constraint (22d) is imposed to prevent the plant from operating in regions that could be potentially unsafe or harmful to the system. By restricting the states within safe operating boundaries, this constraint ensures that the predictive control strategy respects critical process limitations, avoiding conditions that could lead to excessive stress, damage, or unsafe chemical concentrations. Together, these constraints enable the controller to compute optimal inputs that not only achieve the desired control objectives but also respect both the physical and safety limitations of the system, thus ensuring reliable and robust operation of the plant.

Remark 1: **Dealing with numerical problems.** The measurement array defined in (15) comprises quantities spanning several orders of magnitude. While this dependence is inherently linked to the choice of physical units, it may lead to numerical issues from a computational perspective. Although the DMDc-based linear model is still able to predict the system evolution under this condition, the online optimization problem in the MPC scheme may suffer from poor numerical conditioning. For this reason, all measurements are appropriately scaled, and the controller is implemented in the correspondingly scaled lifted space.

V. Simulation

All the introduced equations have been implemented in MATLAB.

Fig. 3 represents the behavior of the digital twin. In particular, it shows the expected free evolution of the plant for 500 min. As expected, the trans-membrane flux naturally decreases, with consequent increasing of the feed concentration and the draw volume. At the same time, the feed volume and the draw concentration decrease.

Fig. 4 illustrates the performance of the proposed **DMDc-based MPC** algorithm, with control horizon $h = 10$. Initially, the desired level of trans-membrane flux is set to $J_w^{ref} = 4 \cdot 10^{-3} mol/m^2/s$. After $100 min$ the set point is set to $J_w^{ref} = 6 \cdot 10^{-3} mol/m^2/s$. The flux adequately tracks the reference signal.

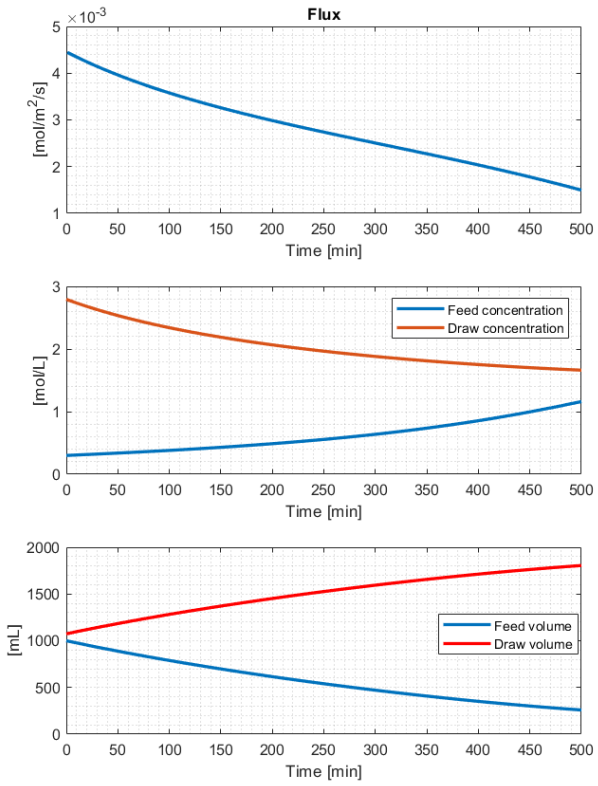

Fig. 3. Expected evolution of the plant computed using the digital twin

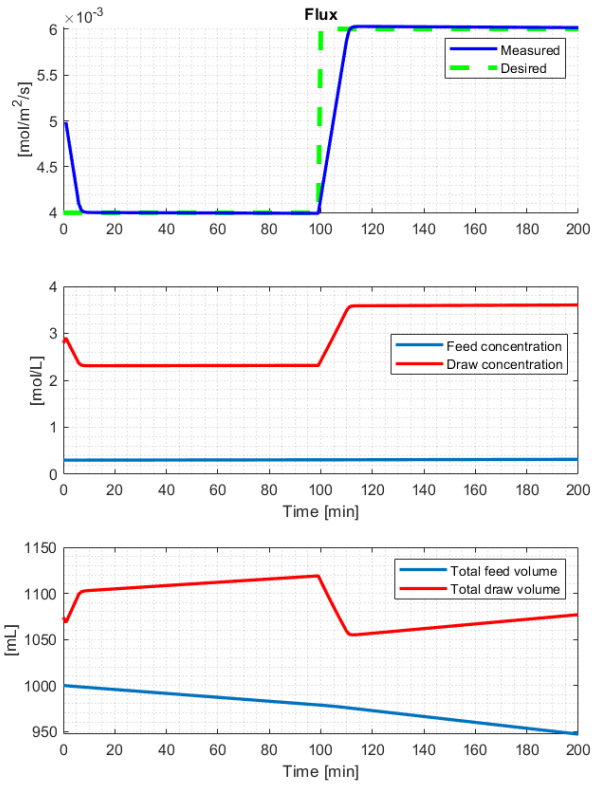

Fig. 4. Controlled evolution of the plant

CONCLUSION

This paper presented a Data-Driven predictive control scheme for the regulation of trans-membrane flux in a membrane-based separation process. A digital twin of the plant has been synthesized combining physicochemical knowledge with data. The Dynamic Mode Decomposition with Control algorithm has been properly integrated with Model Predictive Control to achieve constrained flux regulation.

Numerical results demonstrated that the proposed DMDc-based digital twin provides sufficient predictive accuracy for control purposes and enables effective setpoint tracking across multiple operating conditions. The integration of data-driven modeling and predictive control proved to be a viable strategy for handling the intrinsic nonlinearities of the process without relying on a full first-principles model.

Future research will focus on deploying the proposed control strategy on a micro-controller for real-time implementation and experimental validation, as well as extending the methodology to the control of other similar membrane-based processes.

REFERENCES

[1] S. L. Brunton, J. N. Kutz, "Data-driven science and engineering: Machine learning, dynamical systems, and control," *Cambridge University Press*, 2022.

[2] B. O. Koopman, "Hamiltonian systems and transformation in Hilbert space," *Proceedings of the National Academy of Sciences*, Vol. 17, no. 5, Pp. 315-318, 1931.

[3] I. Mezić, "Spectral properties of dynamical systems, model reduction and decompositions," *Nonlinear Dynamics*, Vol. 41, No. 1, Pp. 309-325, 2005.

[4] I. Mezić, "Analysis of fluid flows via spectral properties of the Koopman operator," *Annual review of fluid mechanics*, Vol. 45, No. 1, Pp. 357-378, 2013.

[5] W. A. Manzoor, S. Rawashdeh, and A. Mohammadi, "Vehicular applications of koopman operator theory—a survey," *IEEE Access*, Vol. 11, Pp. 25917-25931, 2023.

[6] L. Shi, et al, "Koopman operators in robot learning," *IEEE Transactions on Robotics*, 2026.

[7] J. L. Proctor, S. L. Brunton, and J. N. Kutz, "Dynamic mode decomposition with control," *SIAM Journal on Applied Dynamical Systems*, Vol. 15, no. 1, pp. 142-161, 2016.

[8] J. L. Proctor, S. L. Brunton, and J. N. Kutz, "Generalizing Koopman theory to allow for inputs and control," *SIAM Journal on Applied Dynamical Systems*, Vol. 17, no. 1, Pp. 909-930, 2018.

[9] P. J. Schmid, "Dynamic mode decomposition of numerical and experimental data," *Journal of Fluid Mechanics*, Vol. 656, Pp. 5-28, 2010.

[10] E. Drioli, A. Criscuoli, and E. Curcio, "Membrane contactors and catalytic membrane reactors in process intensification," *Chemical Engineering & Technology: Industrial Chemistry-Plant Equipment-Process Engineering-Biotechnology*, Vol. 26, No. 9, Pp.975-981, 2003.

[11] Y. Kumar, et al., "White wine dealcoholization by osmotic distillation: An experimental study and impact on key quality parameters," *Journal of Food Engineering*, Vol. 391, 2025.

[12] N. Rajoub, et al., "A workflow for the development of template-assisted membrane crystallization downstream processing for monoclonal antibody purification," *Nature Protocols*, Vol. 18, No. 10, Pp. 2998-3049, 2023.

[13] F. Borrelli, A. Bemporad, and M. Morari, "Predictive control for linear and hybrid systems," *Cambridge University Press*, 2017.
[14] F. Giannini, and D. Famularo, "A data-driven approach to set-theoretic model predictive control for nonlinear systems," *Information*, Vol. 15, No. 7, 2024.
[15] A. Gharsallaoui, et al, "Relationships between hydration number, water activity and density of aqueous sugar solutions," *Food Chemistry*, Vol. 106, No. 4, Pp. 1443-1453, 2008.
[16] L. A. Romankiw, and I. M. Chou, "Densities of aqueous sodium chloride, potassium chloride, magnesium chloride, and calcium chloride binary solutions in the concentration range 0.5-6.1 m at 25, 30, 35, 40, and 45. degree," *C. Journal of Chemical and Engineering Data*, Vol. 28, No. 3, Pp. 300-305, 1983.